Power Performance and Scalability of AlGaN/GaN Power MODFETs

Egor Alekseev, *Member, IEEE*, Dimitris Pavlidis, *Fellow, IEEE*, Nguyen X. Nguyen, *Member, IEEE*, Chanh Nguyen, *Member, IEEE*, and David E. Grider

***Abstract*—The scalability of power performance of AlGaN/GaN MODFETs with large gate periphery, as necessary for microwave power devices, is addressed in this paper. High-frequency large-signal characteristics of AlGaN/GaN MODFETs measured at 8 GHz are reported for devices with gatewidths from 200 μm to 1 mm. 1-dB gain compression occurred at input power levels varying from -1 to $+10$ dBm as the gatewidth increased, while gain remained almost constant at $\sim$17 dB. Output power density was $\sim$1 W/mm for all devices and maximum output power (29.9 dBm) occurred in devices with 1-mm gates, while power-added efficiency remained almost constant at $\sim$30%. The large-signal characteristics were compared with those obtained by dc and small-signal S-parameters measurements. The results illustrate a notable scalability of AlGaN/GaN MODFET power characteristics and demonstrate their excellent potential for power applications.**

***Index Terms*—Device measurements, microwave power amplifiers, MODFETs, semiconductor.**

I. Introduction

THE emerging wireless applications for commercial and defense use stimulate the growing demand for development of high-power monolithic-microwave integrated-circuit (MMIC) power amplifiers in the 1–30-GHz frequency range. Currently, most power MMICs at these frequencies employ GaAs-based microwave transistors. However, wide-bandgap semiconductors such as III–V nitrides offer a possibility of operation with a higher output power due to increased critical field ($E_{CR} = 2$ MV/cm for GaN and 0.4 MV/cm for GaAs), high carrier saturation velocity ($V_{\rm SAT} = 2 \times 10^7$ cm/s for GaN and 1×10^7 cm/s for GaAs), and good thermal conductivity ($\lambda = 1.3$ W/cm for GaN and 0.5 W/cm for GaAs).

Excellent high-frequency characteristics demonstrated using GaN-based heterojunction field-effect transistors appear to support the high-power potential promised by these devices, and are analyzed in Section II. AlGaN/GaN HEMTs grown on SiC substrates demonstrated record power density at X-band (7 W/mm at 10 GHz) [1], while AlGaN/GaN HEMTs grown on sapphire had 3 W/mm at 18 GHz [2]. Moreover, the use of wide-bandgap semiconductors in power amplifiers not only increases the output power, but also extends the temperature tolerance and radiation hardness of the circuits. The latter is corroborated by recently demonstrated operation of GaN-based HFETs at 750 °C [3].

AlGaN/GaN modulation-doped FETs grown on sapphire by RF-assisted molecular beam epitaxy (MBE) have a high potential for high-power electronics, as previously reported in [4]. The dc and small-signal high-frequency performance of $Al_{0.3}Ga_{0.7}N$/GaN MODFETs with gatewidths ranging from 200 to 800 μm was also recently reported [5], and excellent uniformity of drain current across the wafer and scalability of drain current and transconductance with the gatewidth was demonstrated. However, there is lack of detailed information on the scalability of power saturation characteristics for large gate-periphery power devices. A first analysis of power characteristics and scalability issues in AlGaN/GaN HEMTs was recently reported in [6]. This paper presents further detail on the large-signal performance and scalability of AlGaN/GaN power MODFETs with gatewidths up to 1 mm. Section II reports general power considerations of GaN-based devices compared with GaAs-based designs and describes the design, growth, and geometry details. The dc and small-signal characteristics are presented in Section III. The bias and gatewidth dependence of the large-signal characteristics are described in Sections IV and V, while correlation between dc, RF, and power performance are reported in Section VI.

II. Power Considerations and Devices Used for Large-Signal Studies

An analysis of the power characteristics of the investigated AlGaN/GaN MODFETs was performed first by comparing their performance to that of GaAs-based devices. The power capability of different semiconductor materials can be compared using figures-of-merit that evaluate their power-handling capabilities. Thus, Johnson's $\mathrm{JFOM} = (E_{CR}V_{\rm SAT}/\pi)^2$ measures the maximum capability to energize carriers by electric field [7], while Shenai's figure-of-merit $\mathrm{QF1} = \lambda\sigma_a$ (where λ is the thermal conductivity and σ_a is the conductance of the channel) measures the power handling in terms of generated heat [8]. To illustrate the advantages of nitride technology, these figures-of-merit calculated for GaN and normalized with respect to GaAs are presented in Table I. Whereas the ability of GaN to energize carriers is 100 times better than that of GaAs, its power handling in terms of generated heat varies depending on the choice of substrate.

Shenai's figure-of-merit QF1 is designed to evaluate the power handling under the assumption that the generated heat is removed through a substrate made of the same material

Manuscript received June 8, 1999. This work was supported by Microwave and Analog Front End Technology 3 under Contract N66001-96-C-8637, and by the Office of Naval Research under Contract N00014-92-J-1552 and Contract N00014-99-1-0513).

E. Alekseev and D. Pavlidis are with the Solid-State Electronics Laboratory, Department of Electrical Engineering and Computer Science, The University of Michigan at Ann Arbor, Ann Arbor, MI 48109-2122 USA.

N. X. Nguyen, C. Nguyen, and D. E. Grider are with HRL Laboratories, Malibu, CA 90265 USA.

Publisher Item Identifier S 0018-9480(00)08734-2.

TABLE I
HIGH-POWER CAPABILITY FIGURES-OF-MERIT FOR GaN NORMALIZED TO GaAs

Semiconductor Figures of Merit (FOMs) Normalized to GaAs	GaAs	GaN grown on	
		Sapphire	SiC
Capability to energize carriers (Johnson's JF = $(E_{CR}V_{SAT}/\pi)^2$)	1	100	
Thermal power handling with native substrate (Shenai's QF1= $\lambda\sigma_s$)	1	22	
Thermal power handling with hetero substrate (QFS=$\lambda_{SUB}\sigma_s$)	1	5	76

as the device. However, this is not the case for III–V nitride technology, which is being developed on sapphire and SiC substrates with thermal conductivity of 0.3 and 4.5 W/cm/K, respectively versus 1.3 W/cm/K for GaN. An extended definition of Shenai's figure-of-merit: $\mathrm{QFS} = \lambda_{\mathrm{SUB}}\sigma_a$ is proposed to evaluate the power handling in GaN-based devices by taking into account the thermal conductivity of the substrate material. While a power-handling improvement of 22 (when compared with GaAs) is predicted by QF1 for GaN-based technology, QFS shows that, in the case where GaN-based devices are grown on sapphire, the possible improvement is limited to five times.

The AlGaN/GaN devices studied in this paper consisted of an $Al_{0.3}Ga_{0.7}N$ 50-Å-thick donor layer followed by 30-Å-thick $Al_{0.3}Ga_{0.7}N$ spacer, and a 5000-Å-thick GaN channel. An unintentionally doped 250-Å-thick $Al_{0.3}Ga_{0.7}N$ cap was used for improved contact characteristics, while a GaN thick buffer was employed for improved quality of the materials, which were grown on sapphire substrates. RF-assisted MBE was used for growth. The layer growth and fabrication details of 0.25-μm-long gate MODFETs on such layers have been reported elsewhere [9]. Power devices with two, four, eight, and ten 100-μm-wide gate fingers (maximum width of 1 mm) and a drain–source spacing of 2 μm have been investigated. The thermal effects were reduced by employing 30-μm-thick Au-plated heat sinks.

III. DC AND SMALL-SIGNAL HIGH-FREQUENCY CHARACTERISTICS

Typical I_D–V_{DS} and transfer characteristics of AlGaN/GaN MODFETs are shown in Fig. 1(a) and (b) for a devices with 200-μm gatewidth. The maximum drain current shown for these devices was 500 mA/mm, while their transconductance (g_m) was 100 mS/mm. g_m reached maximum for $V_{\mathrm{GS}} = -5$ V ($V_{\mathrm{DS}} = 7$ V), while both the I_D and g_m remained generally unchanged for V_{DS} between 9 and 25 V when V_{GS} was -5 V. Current-compliance limitation of the semiconductor-parameter analyzer used for obtaining these data did not allow application of gate voltages larger than -2 V. The device pinchoff voltage was -8 V. The ON-state drain–source breakdown was found to be higher than 50 V, while drain current saturation occurred at knee voltage (V_K), as shown in Fig. 1(a).

Small-signal S-parameters of AlGaN/GaN MODFETs with varying gatewidths were measured between 0.5–25.5 GHz. The current–gain cutoff frequency (f_T) and maximum oscillation frequency (f_{MAX}) extrapolated from the S-parameters for different bias conditions are shown in Fig. 2. This figure shows

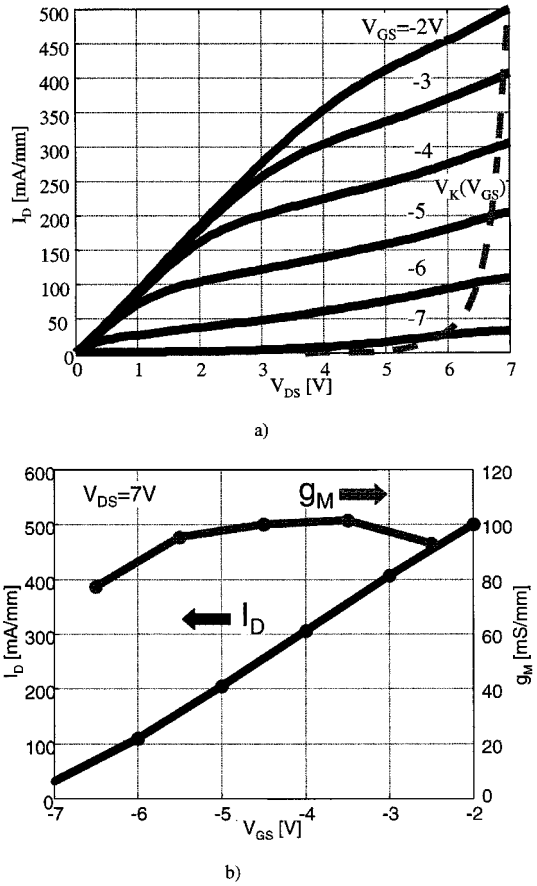

Fig. 1. (a) I_D–V_{DS}. (b) Transfer characteristics of AlGaN/GaN MODFET with 200-μm gatewidth.

that f_T and f_{MAX} were maximum for V_{GS} between -4 and -6 V ($V_{\mathrm{DS}} = 15$ V). f_T and f_{MAX} slowly increased with drain–source voltage for $V_{\mathrm{DS}} > 5$ V when V_{GS} was fixed at -5 V. f_T was 27 GHz for most devices, while f_{MAX} varied from 45 to 70 GHz.

Small-signal S-parameters were also used to extract equivalent-circuit elements under optimal biasing conditions ($V_{\mathrm{DS}} = 15$ V and $V_{\mathrm{GS}} = -5$ V). The values of equivalent-circuit elements obtained by circuit optimization in microwave simulator Libra are listed in Table II. The contact resistance of 0.5 $\Omega \cdot$ mm obtained from transmission-line matrix (TLM) measurements [10] was in agreement with the high-frequency source and drain resistance (R_D and R_S) obtained by fitting the S-parameter data. The extrinsic RF transconductance demonstrated notable scaling with the gatewidth ($g_m \approx 100$ mS/mm) and agreed well with the transconductance extracted from dc measurements across a wide range of gate–source voltages, as shown in Fig. 3. Although the exact features of the devices at intermediate frequencies are not known at this stage, the agreement between the dc and RF values of transconductance suggest the presence of limited frequency dispersion under small-signal excitation. g_m dispersion with frequency is usually associated with the presence of traps in the channel or at the channel-barrier interface, as shown in previous reports on other types of heterostructure FETs [11]. The variations in the time response of traps cause may cause transconductance values under RF exci-

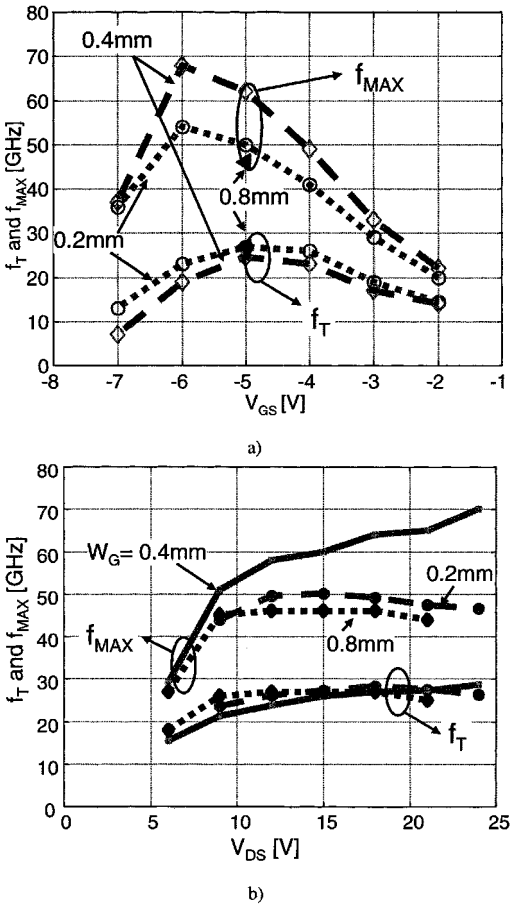

Fig. 2. Bias dependence of f_{MAX} and f_T for AlGaN/GaN MODFETs with various gatewidths.

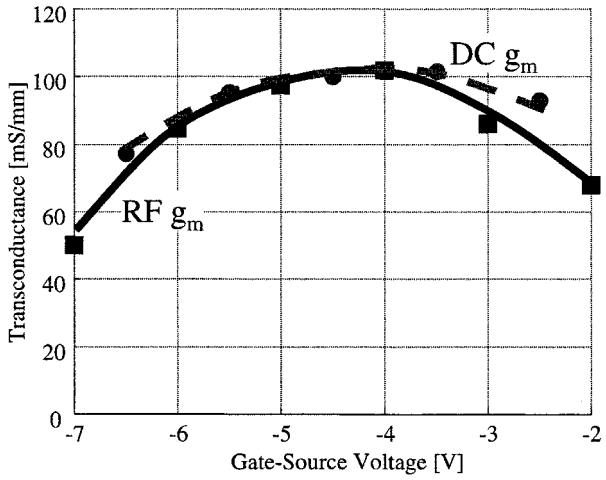

Fig. 3. Dependence of dc and RF transconductance on V_{GS} for 0.2-mm AlGaN/GaN MODFETs.

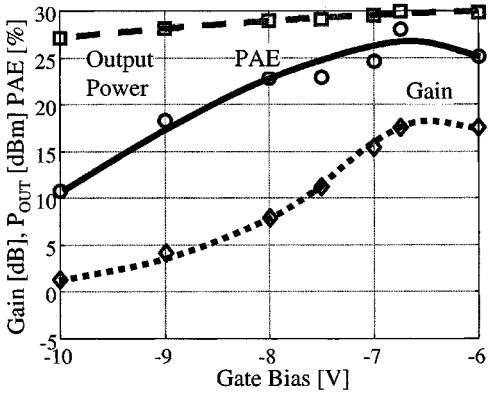

Fig. 4. Dependence of gain, output power, and PAE on gate bias of AlGaN/GaN MODFET with 1-mm gatewidth.

TABLE II
HIGH-FREQUENCY SMALL-SIGNAL EQUIVALENT-CIRCUIT PARAMETERS OF MODFETS ($V_{\mathrm{DS}} = 15$ V AND $V_{\mathrm{GS}} = -5$ V)

Width [μm]	I_D [mA]	g_m [mS]	C_{GS} [fF]	C_{GD} [fF]	C_{DS} [fF]	R_{DS} [Ω]	R_t [Ω]	τ [ps]
200	36	19	106	25	95	1095	10	1.7
400	52	35	220	47	187	391	7	2.4
800	130	83	412	102	297	136	1.7	1.9

tation, which are smaller than under dc conditions. The excellent agreement of dc and high-frequency extracted transconductance values observed in this paper supports the fact that these AlGaN/GaN layers grown by RF-assisted MBE allow realization of devices with minimum small-signal dispersion effects, as discussed more extensively in Section VI. Characteristics of this type are of prime importance in obtaining good high-frequency and power performance from GaN FETs. These features are in contrast with observations by others on MOCVD-grown GaN-based devices [12], [13].

It was also observed that the output drain–source capacitance C_{DS}, the input gate–source capacitance C_{GS}, and the feedback drain–source capacitance C_{GD} also scale linearly with the gatewidth. The values of C_{GD}, C_{GS}, and C_{DS} capacitance are 120, 540, and 440 fF/mm, respectively. This good scalability of the devices is very important for circuit-design applications.

IV. BIAS DEPENDENCE OF LARGE-SIGNAL CHARACTERISTICS

An automatic on-wafer load–pull system with electromechanical tuners has been employed to obtain P_{OUT}-P_{IN} characteristics of GaN-based MODFETs at 8 GHz. Both source and load tuners were positioned to obtain best matching and, therefore, maximum gain at an input power level corresponding to ∼1-dB gain compression. The bias dependence of output power, power-added efficiency (PAE), and gain was investigated first as a function of gate bias for fixed drain bias $V_{\mathrm{DS}} = 21$ V. Devices with 1-mm gatewidth demonstrated maximum output power (30 dBm), PAE (28%), and gain (17.6 dB) when the gate bias was set to -7 V, as shown in Fig. 4. Limitations imposed by current handling of the microwave probes and bias tees used in characterization did not allow reducing the gate bias ($|V_{\mathrm{GS}}|$) below 6 V as this led to drain current in excess of 500 mA. The maximum output power and large-signal performance is, therefore, expected to be higher than described by the results of Fig. 4.

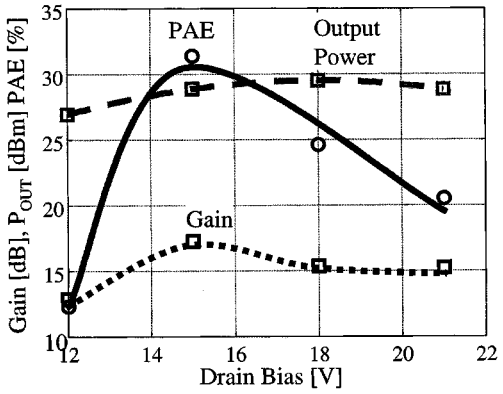

Fig. 5. Dependence of gain, output power, and PAE on drain bias of AlGaN/GaN MODFET with 1-mm gatewidth.

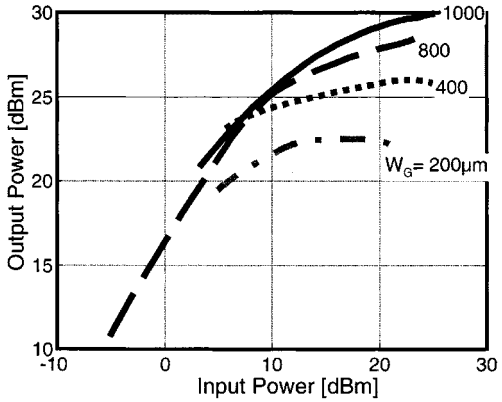

Fig. 6. Power saturation characteristics of AlGaN/GaN MODFETs as a function of gatewidth.

The dependence of output power, PAE, and gain of 1-mm gate devices on the drain bias was also investigated, and is shown in Fig. 5. For these tests, the gate bias was kept constant at −5 V. Maximum PAE (32%) was obtained for drain bias of 15 V, while maximum output (30 dBm) occurred at 18 V. Thermal effects are suggested as a cause for reduced efficiency and output power at drain bias exceeding 18 V.

V. Gatewidth Dependence of Large-Signal Characteristics

The dependence of power performance on the gatewidth was investigated using AlGaN/GaN MODFETs with two, four, eight, and ten 100-μm-wide gate fingers. All devices were first biased for maximum gain at an input power level corresponding to ∼1-dB gain compression and load terminations corresponding to small-signal matching conditions. The source and load tuners were then adjusted to improve matching and maximize the gain.

$P_{\rm OUT}$–$P_{\rm IN}$ characteristics of devices with different gatewidths are shown in Fig. 6. Biasing conditions, gain, output power, and PAE are listed in Table III. Typical power gain of ∼17 dB and output power density of ∼1 W/mm were obtained for devices with 200–1000 μm gatewidths at 8 GHz. The largest output power of 29.9 dBm (1 W/mm) with associated gain of 4 dB was obtained for devices with 1-mm gatewidth.

The scalability of AlGaN/GaN MODFET power characteristics is illustrated in Fig. 7. Devices with wider gates showed delayed onset of gain compression, as demonstrated by higher input power at 1-dB gain compression $P_{\rm IN1dB}$ for gatewidths up to 800 μm. When the width is increased from 200 to 800 μm, $P_{\rm IN-1dB}$ is increased from −1 to 10 dBm, $P_{\rm OUT1dB}$ is increased from 20 to 25 dBm, and $P_{\rm OUTMAX}$ is increased from 23 to 30 dBm. The output power density (∼1 W/mm), PAE (∼30%), and gain (∼17 dB) remained constant. $P_{\rm IN1dB}$ and $P_{\rm OUT1dB}$ showed a small decrease in 1-mm devices compared with 800-μm MODFETs. This is probably caused by the limitations in current handling described earlier, which did not allow operation of the 1-mm devices at their maximum power capacity.

TABLE III
Power Saturation Characteristics of AlGaN/GaN Power Modfets for Various Gatewidths

Width [μm]	V_{DS} [V]	I_D [A/mm]	V_{GS} [V]	Gain [dB]	P_{IN-1dB} [dBm]	Max P_{OUT} [dBm]	P_{OUT} [W/mm]	PAE_{-1dB} [%]
200	15	170	-4.5	15.9	-0.8	22.5	0.89	30.3
400	12	222	-4.5	17.4	3.2	26.0	1.00	28.9
800	12	186	-5.0	15.9	10.3	28.5	0.87	31.5
1000	18	168	-6.75	17.6	7.3	29.9	0.99	28.1

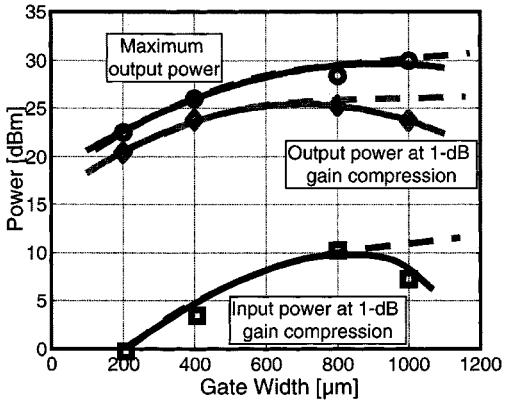

Fig. 7. Scalability of AlGaN/GaN MODFET power characteristics shown by the dependence of output and input power at 1-dB gain compression on gatewidth.

Constant output power ($P_{\rm OUT}$) and constant PAE contours of AlGaN/GaN MODFETs were evaluated using the load–pull system and allowed to obtain loading conditions for maximum output power as necessary for circuit design. The contours of AlGaN/GaN MODFET with 800-μm gate under high-input power conditions ($P_{\rm IN}$ = 22 dBm) are shown in Fig. 8. The contours were found to remain circular up to power levels corresponding to severe gain compression (∼10 dB). Moreover, when the load impedance was positioned for maximum $P_{\rm OUT} = 28$ dBm, the value of (30%) was close to its maximum value of 32%, and the two optimal loads were located near each

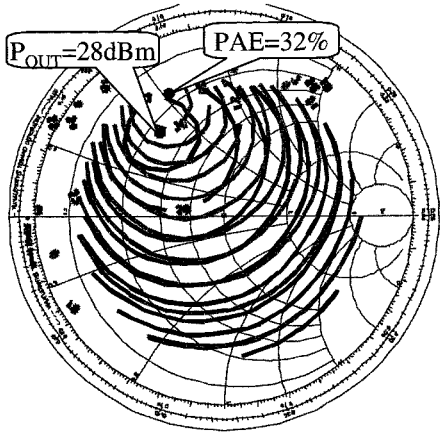

Fig. 8. Constant output power ($P_{\rm OUT}$) and constant PAE contours for AlGaN/GaN MODFET with 800-μm gatewidth under $P_{\rm IN} = 22$ dBm, $V_{\rm DS} = 12$ V, $V_{\rm GS} = -5$ V.

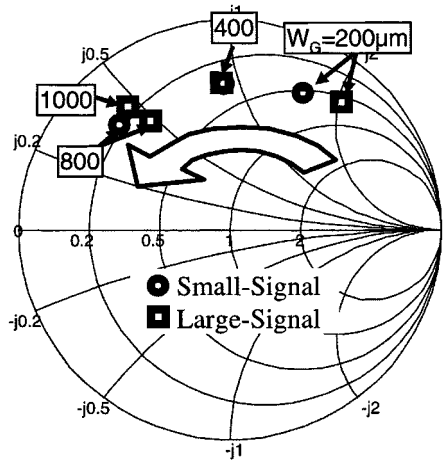

Fig. 9. Dependence of small- and large-signal output impedance of AlGaN/GaN MODFETs on gatewidths.

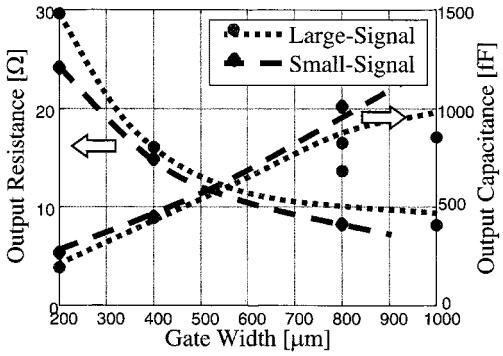

Fig. 10. Small- and large-signal values of the output capacitance and output resistance as a function of gatewidth.

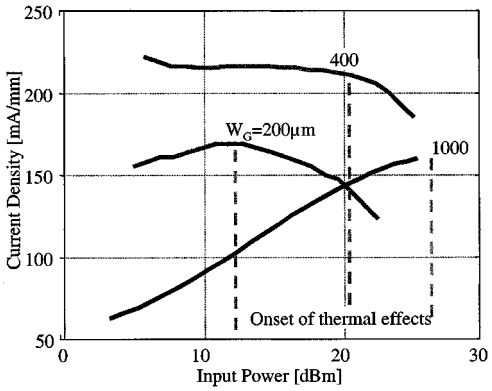

Fig. 11. Dependence of self-biased drain current on input power measured during power saturation measurements of AlGaN/GaN MODFETs with various gatewidths.

other on the Smith chart. This positive feature does not necessarily occur in all devices and suggests a possibility of Class-A/AB power-amplifier realization without a considerable tradeoff between output power and PAE. Studies of the other classes of operation including harmonic tuning are beyond the scope of work reported in this paper.

VI. Correlation Between DC, RF, and Power Characteristics

Source–pull and load–pull techniques were used to determine the large-signal output impedance of the AlGaN/GaN MODFETs. The output impedance of the devices was determined by the position of the complex conjugate of the optimal load on the Smith Chart. The dependence of the optimal loads under large-signal conditions on the gatewidth is shown with squares in Fig. 9. They are in good agreement with the positions of optimal loads under small-signal conditions calculated from small-signal S-parameters, indicated in Fig. 9 with circles. When the gatewidth is increased from 200 μm to 1 mm, the optimal load moved as expected along a line corresponding to increased output capacitance and decreased output resistance.

It was observed that not only the small-signal, but also the large-signal output capacitance scale linearly with the gatewidth. This good scalability is very important for circuit design applications. Moreover, the large-signal output capacitance and resistance were in good agreement with the small-signal values extracted by fitting to S-parameters, as shown in Fig. 10.

It is also important to note that the AlGaN/GaN MODFETs of this paper demonstrated the same value of transconductance $g_m \approx 100$ mS/mm, both at dc and RF, which suggests the absence of undesirable frequency dispersion effects. As mentioned earlier, this impacts positively the high frequency and power performance. To validate this prediction, the output power density obtained during load–pull characterization (RF $P_{\rm OUT}$) was compared with the output power density predicted from dc measurements (DC $P_{\rm OUT}$).

The maximum allowed voltage $V_{\rm MAX}$ and current $I_{\rm MAX}$ swings considered for this purpose were based on the biasing conditions used for evaluation of the reported power characteristics: $V_{\rm MAX} = 2 \times V_{\rm DS} - V_K$, where $V_{\rm DS}$ and V_K are the

TABLE IV
COMPARISON OF DC PREDICTED AND RF MEASURED OUTPUT POWER DENSITY OF AlGaN/GaN MODFETS

Width [μm]	V_{DS} [V]	I_D [A/mm]	RF-P_{OUT} [W/mm]	DC-P_{OUT} [W/mm]	RF-P_{OUT}/DC-P_{OUT} [%]
200	15	170	0.89	0.97	91
400	12	222	1.00	0.94	105
800	12	186	0.87	0.79	109
1000	18	168	0.99	1.16	85

drain–source bias and the knee voltage of the MODFET, respectfully, and $I_{\rm MAX} = 2 \times I_D$, where I_D is the value of the drain current under large-signal excitation obtained during RF power measurements. The use of a large-signal experimental value of I_D for representing the amplitude of the RF swing is justified by the dependence of $P_{\rm OUT}$ on $V_{\rm GS}$ (see Fig. 4). $P_{\rm OUT}$ is decreased for larger negative $V_{\rm GS}$ indicating that the RF swing of I_D is affected by the biasing conditions. The experimental value of I_D is, therefore, a better choice than a value of $I_{\rm DSS}$ based on extraction from dc measurements only.

The dependence of I_D on $P_{\rm IN}$ for AlGaN/GaN MODFETs with various gatewidths is shown in Fig. 11. The biasing conditions at low $P_{\rm IN}$ varied between 150 mA/mm (Class AB) for 0.2 mm, 230 mA/mm (Class A) for 0.4 mm, and 75 mA/mm (Class B) for a 1-mm MODFET, respectively. When the input power is increased, I_D increases toward $I_{\rm DSS}/2$, as expected for devices biased in Classes AB and B, while it remains constant for the device in Class A. The decrease of I_D at high power levels is attributed to thermal effects since the input power level where thermal effects become dominant (see Fig. 11) scales with the device area.

These conditions allowed calculation of dc $P_{\rm OUT} = I_{\rm MAX} \times V_{\rm MAX}/8$. The results of the comparison are presented in Table IV. The values of the RF output power density are very close to the dc output power density. The results show an exceptionally good correlation of AlGaN/GaN MODFET dc, RF, and power characteristics, and demonstrate their excellent potential for power applications.

VII. CONCLUSIONS

Overall, AlGaN/GaN power MODFETs with gatewidths up to 1 mm have been characterized using an automatic load–pull system. High output power (29.9 dBm) with high PAE (32%) was obtained from discrete devices with 1-mm gatewidth. The optimal loads for output power and efficiency were located close to each other as necessary for power-amplifier applications. Excellent scalability of small- and large-signal characteristics was observed for devices with gatewidths varying from 200 μm to 1 mm. Good output power and PAE were obtained from discrete AlGaN/GaN MODFETs grown on sapphire, indicating the high potential of GaN-based technology for power applications. Good correlation is demonstrated between dc, RF, and power characteristics as desired for circuit design applications and optimum performance of microwave power devices.

REFERENCES

[1] S. T. Sheppard *et al.*, "High power microwave GaN/AlGaN HEMT's on semi-insulating silicon carbide substrates," *IEEE Electron Devices Lett.*, vol. 20, pp. 161–163, Apr. 1999.

[2] U. K. Mishra, Y.-F. Wu, B. P. Keller, S. Keller, and S. P. Denbaars, "GaN microwave electronics," *IEEE Trans. Microwave Theory Tech.*, vol. 46, pp. 756–761, June 1998.

[3] I. Daumiller, C. Kirchner, M. Kamp, K. J. Ebeling, L. Pond, C. E. Weitzel, and E. Kohn, "Evaluation of AlGaN/GaN HFET's up to 750 °C," in *Device Res. Conf. Dig.*, 1998, pp. 114–115.

[4] Y. F. Wu *et al.*, "Short-channel $Al_{0.5}Ga_{0.5}N$/GaN MODFET's with power density >3 W/mm at 18 GHz," *Electron. Lett.*, vol. 33, no. 20, pp. 1742–1743, 1997.

[5] N. X. Nguyen *et al.*, "Device characteristics of scaled GaN/AlGaN MODFETs," *Electron. Lett.*, vol. 34, no. 8, pp. 811–812, 1998.

[6] E. Alekseev, D. Pavlidis, N. X. Nguyen, C. Nguyen, and D. E. Grider, "Large-signal characteristics of AlGaN/GaN power MODFETs," in *IEEE MTT-S Int. Microwave Symp. Dig.*, vol. 2, 1999, pp. 533–536.

[7] E. O. Johnson, "Physical limitations on frequency and power parameters of transistors," *RCA Rev.*, vol. 26, pp. 163–177, 1965.

[8] K. Shenai, R. S. Scott, and B. J. Baliga, "Optimum semiconductors for high-power electronics," *IEEE Trans. Electron Devices*, vol. 36, pp. 1811–1823, Sept. 1989.

[9] N. X. Nguyen *et al.*, "GaN/AlGaN MODFET with 80 GHz $f_{\rm MAX}$ and > 100 V gate–drain breakdown voltage," *Electron. Lett.*, vol. 33, no. 4, pp. 334–335, 1997.

[10] C. Nguyen, N. X. Nguyen, M. Le, and D. E. Grider, "High performance GaN/AlGaN MODFET's grown by RF-assisted MBE," *Electron. Lett.*, vol. 34, no. 3, pp. 309–311, Feb. 1998.

[11] Y. J. Chen and D. Pavlidis, "Low-frequency noise and frequency dispersion characteristics of GaInP/GaAs and AlGaAs/GaAs HEMTs," in *Proc. Int. Semiconduct. Device Res. Symp.*, 1991, pp. 677–680.

[12] W. Kruppa, S. C. Binari, and K. Doverspike, "Low-frequency dispersion characteristics of GaN HFETs," *Electron. Lett.*, vol. 31, no. 22, pp. 1951–1952, Oct. 26, 1995.

[13] M. A. Khan, M. Shur, J. N. Kuznia, Q. Chen, J. Burm, and W. Schaff, "Temperature-activated conductance in GaN/AlGaN heterostructure field-effect transistors operating up to 300 °C," *Appl. Phys. Lett.*, vol. 66, no. 9, pp. 1083–1085, Feb. 27, 1995.

Egor Alekseev (S'94–M'00) received the Engineer–Researcher–Scientist degree with a specialization in materials and components of modern microelectronics from the St.-Petersburg State Technical University (former Polytechnic Institute), St.-Petersburg, Russia, in 1992, and the M.S. and Ph.D. degrees in electrical engineering from The University of Michigan at Ann Arbor, in 1995 and 2000, respectively. His undergraduate research on InP-based MOS structures was conducted at the Ioffe Physico-Technical Institute, St.-Petersburg, Russia.

Since 1994, he has been a Graduate Student Research Assistant in the Solid State Electronics Laboratory, The University of Michigan at Ann Arbor, where his concentration was in the areas of InP- and GaN-based devices for signal control and generation. His is currently a Research Fellow in the Solid State Electronics Laboratory, where he is involved with III–V nitrides for high-power and high-frequency applications.

Dimitris Pavlidis (S'73–M'76–SM'83–F'93) received the B.Sc. degree in physics from the University of Patras, Patras, Greece, in 1972, and the Ph.D. degree in applied science/electronic engineering from the University of Newcastle, Newcastle-upon-Tyne, U.K., in 1976.

He was an Invited Guest at the Institute of Semiconductor Electronics, Technical University of Aachen, Aachen, Germany, in 1974. From 1976 to 1978, he continued as Post-Doctoral Fellow at the University Newcastle-upon-Tyne, where he was engaged in work on microwave semiconductor devices and circuits. In 1978, he joined the High Frequency Institute, Technical University of Darmstadt, Darmstadt, Germany, as a Lecturer, where he was involved with III–V devices and established a new semiconductor technology facility. In 1980, he joined the Central Electronic Engineering Research Institute, Pilani, India, as UNESCO Consultant. From 1980 to 1985, he was an Engineer and Manager of the GaAs Monolithic Microwave Integrated Circuits Department, Thomson-CSF, Corbeville, France, where he was responsible for projects on various monolithic circuits, their technology, and process evaluation. From January to June 1993, he was a Visiting Scientist at the Centre National d'Études des Télécommunications (CNET)/France Telecom, Bagneux, France. Since 1986, he has been involved in research on heterostructure devices and materials at The University of Michigan at Ann Arbor. This includes the design, fabrication, and characterization of GaAs, InP-based HEMTs and heterojunction bipolar transistors (HBTs), diodes for switching and mixing, GaN-based HFETs, and two-terminal devices.

Prof. Pavlidis was the recipient of the 1990 European Microwave Prize for his work in InP-based monolithic integrated HEMT amplifiers, the 1991 decoration of "Palmes Académiques" in the order of Chevalier by the French Ministry of Education for his work in education, the 1992 and 1999 recipient of the Japan Society of Promotion of Science Fellowship for Senior Scientists/Professors presented by the Japanese Government, and the 1992 Humboldt Research Award for Distinguished Senior U.S. Scientists. He was also the recipient of the 1994 University of Michigan Electrical Engineering and Computer Science and 1996 College of Engineering Research Excellence Awards.

Nguyen X. Nguyen (S'89–M'90), photograph and biography not available at time of publication.

Chanh Nguyen (S'92–M'93), photograph and biography not available at time of publication.

David E. Grider, photograph and biography not available at time of publication.